AWZ1066S, a highly specific anti-*Wolbachia* drug candidate for a short-course treatment of filariasis

W. David Hong[a,b], Farid Benayoud[c], Gemma L. Nixon[a], Louise Ford[b], Kelly L. Johnston[b], Rachel H. Clare[b], Andrew Cassidy[b], Darren A. N. Cook[b], Amy Siu[c], Motohiro Shiotani[d], Peter J. H. Webborn[e,1], Stefan Kavanagh[e], Ghaith Aljayyoussi[b], Emma Murphy[b], Andrew Steven[b], John Archer[b], Dominique Struever[f], Stefan J. Frohberger[f], Alexandra Ehrens[f], Marc P. Hübner[f], Achim Hoerauf[f], Adam P. Roberts[b], Alasdair T. M. Hubbard[b], Edward W. Tate[g], Remigiusz A. Serwa[g], Suet C. Leung[a,b], Li Qie[a], Neil G. Berry[a], Fabian Gusovsky[c], Janet Hemingway[h,2], Joseph D. Turner[b], Mark J. Taylor[b], Stephen A. Ward[b,2], and Paul M. O'Neill[a,2]

[a]Department of Chemistry, University of Liverpool, L69 7ZD Liverpool, United Kingdom; [b]Research Centre for Drugs and Diagnostics, Department of Parasitology, Liverpool School of Tropical Medicine, L3 5QA Liverpool, United Kingdom; [c]Eisai AiM Institute, Eisai, Inc., Andover, MA 01810; [d]Drug Safety, Eisai Co., Ltd., 300-2635 Tsukuba, Japan; [e]Drug Safety & Metabolism, IMED Biotech Unit, AstraZeneca UK, CB2 0AA Cambridge, United Kingdom; [f]Institute for Medical Microbiology, Immunology and Parasitology, University Hospital Bonn, 53127 Bonn, Germany; [g]Department of Chemistry, Imperial College London, SW7 2AZ London, United Kingdom; and [h]Department of International Health, Liverpool School of Tropical Medicine, L3 5QA Liverpool, United Kingdom

Contributed by Janet Hemingway, November 9, 2018 (sent for review September 27, 2018; reviewed by David A. Baker, John Horton, and Dennis E. Kyle)

Onchocerciasis and lymphatic filariasis are two neglected tropical diseases that together affect ∼157 million people and inflict severe disability. Both diseases are caused by parasitic filarial nematodes with elimination efforts constrained by the lack of a safe drug that can kill the adult filaria (macrofilaricide). Previous proof-of-concept human trials have demonstrated that depleting >90% of the essential nematode endosymbiont bacterium, *Wolbachia*, using antibiotics, can lead to permanent sterilization of adult female parasites and a safe macrofilaricidal outcome. AWZ1066S is a highly specific anti-*Wolbachia* candidate selected through a lead optimization program focused on balancing efficacy, safety and drug metabolism/pharmacokinetic (DMPK) features of a thienopyrimidine/quinazoline scaffold derived from phenotypic screening. AWZ1066S shows superior efficacy to existing anti-*Wolbachia* therapies in validated preclinical models of infection and has DMPK characteristics that are compatible with a short therapeutic regimen of 7 days or less. This candidate molecule is well-positioned for onward development and has the potential to make a significant impact on communities affected by filariasis.

onchocerciasis | lymphatic filariasis | anti-*Wolbachia* | drug discovery | macrofilaricide

Onchocerciasis (river blindness) and lymphatic filariasis (elephantiasis) continue to inflict serious public health problems throughout tropical communities, globally affecting more than 38 million and 120 million people, respectively. These two neglected tropical diseases are caused by the parasitic filarial nematodes *Onchocerca volvulus* (onchocerciasis), *Wuchereria bancrofti*, *Brugia malayi*, and *Brugia timori* (lymphatic filariasis) (1). Global programs for control and elimination have been developed, but existing approaches target only microfilariae and require prolonged delivery with high treatment coverage to break the transmission cycle of the long-lived adult worm (2, 3). This inability of current drugs to kill adult parasites has highlighted the need for new macrofilaricidal drugs.

Wolbachia are essential for multiple components of filarial nematode biology including larval growth, development, embryogenesis, and, ultimately, survival of many filarial nematodes, including the causative parasites of onchocerciasis and lymphatic filariasis, making this symbiont a validated chemotherapeutic target (4, 5). Although the macrofilaricidal activity of doxycycline through depletion of *Wolbachia* has been proven clinically (6–12), protracted treatment regimens (≥28 d) and contraindications restrict its widespread implementation (13, 14).

Results

Lead Optimization Led to the Selection of AWZ1066S as a Preclinical Candidate. To identify novel anti-*Wolbachia* chemotypes, we screened 10,000 compounds selected from the BioFocus SoftFocus library using a phenotypic cell-based screen incorporating a *Wolbachia*-infected *Aedes albopictus* cell line [C6/36 (wAlbB)] as reported previously (15). From this screen, we identified and confirmed 50 anti-*Wolbachia* active hits (0.5% hit rate) that clustered into six unique chemotypes. Based on an evaluation of drug-like properties and potency, we selected a series of thienopyrimidines for medicinal chemistry optimization. Through a highly integrated academic–industrial partnership, multiparameter lead optimization was performed with over 300 analogs synthesized and assessed for both anti-*Wolbachia* activity and drug metabolism/pharmacokinetic (DMPK) properties [partition coefficient (LogD), aqueous solubility, plasma protein

Significance

Onchocerciasis (river blindness) and lymphatic filariasis (elephantiasis) are neglected tropical diseases that cause severe disability and affect more than 157 million people globally. Current control efforts are hindered by the lack of a safe macrofilaricidal drug that can eliminate the parasitic adult nematodes safely. A clinically validated approach for delivering macrofilaricidal activity is to target the *Wolbachia* bacterial endosymbiont of the causative nematodes. This first-in-class and highly potent and specific anti-*Wolbachia* preclinical candidate molecule, AWZ1066S, has the potential to significantly impact current global onchocerciasis and lymphatic filariasis elimination programs and reduce elimination time frames from decades to years.

Author contributions: W.D.H., A.P.R., E.W.T., F.G., J.H., J.D.T., M.J.T., S.A.W., and P.M.O. designed research; W.D.H., F.B., K.L.J., R.H.C., A.C., D.A.N.C., A. Siu, M.S., G.A., E.M., A. Steven, J.A., D.S., S.J.F., A.E., M.P.H., A.T.M.H., and R.A.S. performed research; W.D.H., F.B., S.C.L., and L.Q. contributed new reagents/analytic tools; W.D.H., G.L.N., L.F., K.L.J., R.H.C., P.J.H.W., S.K., D.S., M.P.H., A.H., A.P.R., E.W.T., N.G.B., F.G., J.D.T., M.J.T., S.A.W., and P.M.O. analyzed data; and W.D.H., J.H., J.D.T., M.J.T., S.A.W., and P.M.O. wrote the paper.

Reviewers: D.A.B., London School of Hygiene & Tropical Medicine; J.H., Tropical Projects; and D.E.K., University of Georgia.

Conflict of interest statement: An international patent (WO2018134685) that includes chemical compounds described in this manuscript has been filed by the authors (W.D.H., F.B., M.J.T., P.M.O., and S.A.W.). Some authors (F.B., A. Siu, M.S., and F.G.) of this manuscript are full-time employees of Eisai, Inc.

This open access article is distributed under Creative Commons Attribution-NonCommercial-NoDerivatives License 4.0 (CC BY-NC-ND).

[1]Present address: PJHW Consultancy Ltd., Macclesfield, SK11 9HD Cheshire, United Kingdom.

[2]To whom correspondence may be addressed. Email: janet.hemingway@lstmed.ac.uk, steve.ward@lstmed.ac.uk, or pmoneill@liverpool.ac.uk.

This article contains supporting information online at www.pnas.org/lookup/suppl/doi:10.1073/pnas.1816585116/-/DCSupplemental.

Published online January 7, 2019.

binding, microsomal and hepatocyte stability] in vitro (16). In this process, we transformed the thienopyrimidine core of the starting hit molecule into quinazoline AWB158 and eventually azaquinazoline AWZ1066, resolving the metabolic weakness associated with the original scaffold while improving potency. Optimization of the 2-position of the azaquinazoline core led to AWZ1066, which was selected as a front runner (Fig. 1*A*; see *SI Appendix*, Fig. S1 for detailed structure–activity relationship analyses of this series). AWZ1066 (racemic mixture) was active against *Wolbachia* in a cell-based assay (17) with an EC_{50} of 2.6 ± 0.5 nM (Fig. 1*B*). In an orthogonal secondary in vitro assay utilizing microfilariae (mf) of the human parasite *B. malayi*, AWZ1066 reduced *Wolbachia* within the mf with an EC_{50} of 150 nM while having no effect on the viability and motility of the mf at up to the top testing concentration of 5 μM.

Specific structural features of AWZ1066, such as the lipophilic electron-withdrawing CF_3 group in the 4-position side chain, the nitrogen at the 8-position of the azaquinazoline core, and the methyl group in the 2-position of the morpholinyl side chain, contribute significantly to potency in both assays (*SI Appendix*, Fig. S1). Matched-pair analyses with or without these individual structural features demonstrated a 10- to 100-fold potency loss. AWZ1066 has two enantiomers, namely AWZ1066S and AWZ1066R, demonstrating minor differences in anti-*Wolbachia* potency in vitro, with the (*S*)-isomer, AWZ1066S, the more potent of the enantiomers in both in vitro assays (EC_{50}: cell assay: 2.5 ± 0.4 vs. 14.4 ± 3.7 nM; microfilaria assay: 121 vs. 408 nM) (Fig. 1*C*). The predicted cost of goods for AWZ1066 and its enantiomers is considered to be low based on two simple sequential amination steps from the readily available 2,4-dichloropyrido[2,3-d] pyrimidine (*SI Appendix*, Fig. S1). This will support cost-efficient large-scale synthesis.

Extensive comparative analysis of the two enantiomers led to the selection of the (*S*)-enantiomer, AWZ1066S, as the preclinical candidate based on superiority in terms of in vitro potency, in vivo efficacy, and safety pharmacology (vide infra).

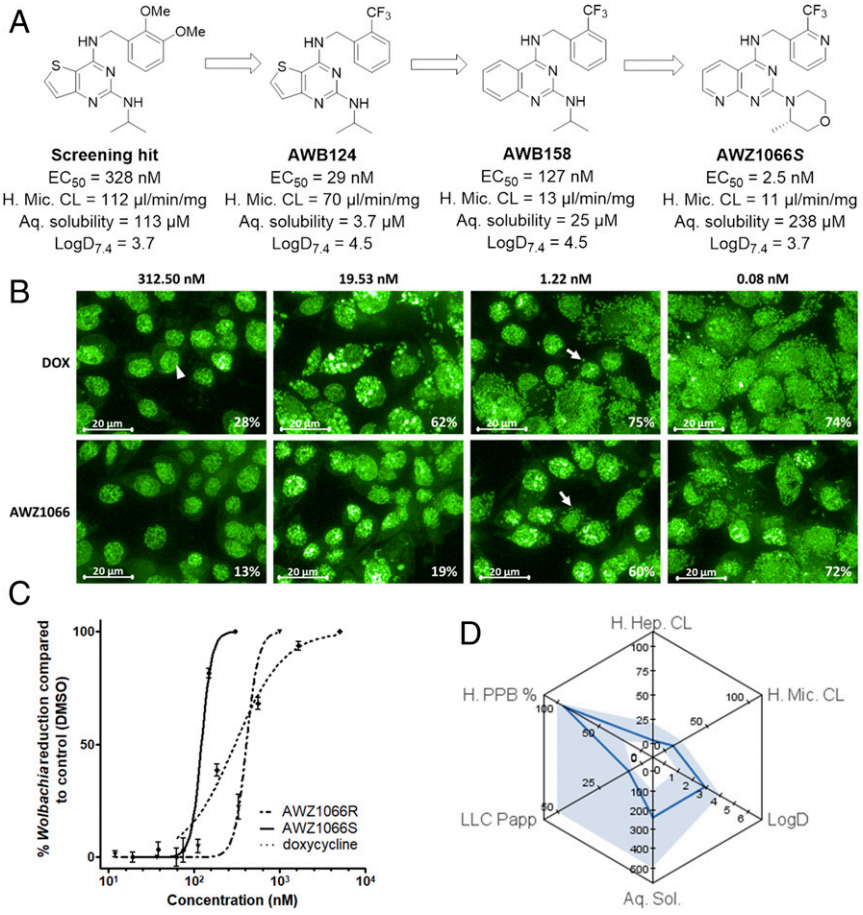


Fig. 1. Medicinal chemistry optimization to identify AWZ1066S, including in vitro potency and DMPK properties. (*A*) Progression of the thienopyrimidine screening hit to the azaquinazoline candidate AWZ1066S through multiparameter optimization to improve potency and DMPK properties. (*B*) AWZ1066 treatment causes a dose-dependent reduction of *Wolbachia* from *Wolbachia*-infected cells. Images are visual representations of cells treated with doxycycline (*Top*) and AWZ1066 (*Bottom*) at various concentrations. In the cell-based assay, C6/36 (*w*AlbB) cells are incubated with compounds and then stained with SYTO11 stain, which stains cell nuclei (large, bright areas; arrowhead) and *Wolbachia* (small, bright punctate staining; arrows) green. Automated capture and imaging analysis is conducted by Operetta and Harmony software (PerkinElmer) (six fields per well, two wells per concentration), which generates "percentage of infected cells" values (shown in white; typical vehicle-treated cells have 70 to 80% infection, while doxycycline at maximum effect has 10 to 15% infection) that are used to calculate the effective concentration of 50% inhibition of *Wolbachia* (EC_{50}: doxycycline 20 nM; AWZ1066 2.6 nM). (*C*) Anti-*Wolbachia* activity of AWZ1066S in the microfilaria assay (EC_{50} 121 nM) in comparison with the (*R*)-isomer, AWZ1066R (EC_{50} 408 nM). Doxycycline was used as positive control (EC_{50} 300 nM). Data are expressed as mean ± SD of five replicates for each concentration. (*D*) In vitro DMPK-related data of AWZ1066S presented in a radar plot. Six axes represent human hepatocyte clearance (μL·min^{-1} 1 × 10^6 cells^{-1}) (H. Hep. CL), human microsome clearance (μL·min^{-1}·mg^{-1}) (H. Mic. CL), $LogD_{7.4}$ (LogD), aqueous solubility in pH 7.4 PBS buffer (μM) (Aq. Sol.), permeability in LLC-PK1 cell assay (1 × 10^6 cm/s) (LLC Papp), and human plasma protein binding (%) (H. PPB). The light blue-shaded area indicates the desired DMPK property target ranges for oral administration.

Pharmacokinetics, Pharmacodynamics, and Safety Profiles of AWZ1066S Match the Anti-*Wolbachia* Macrofilaricide Target Candidate Profile. A key criterion for anti-*Wolbachia* macrofilaricides is the need for oral drug delivery, necessitating good aqueous solubility and metabolic stability. AWZ1066S meets the desired physicochemical properties with acceptable solubility in both PBS buffer (238 μM) and fasted state-simulated intestinal fluid (0.56 mg/mL), moderate human plasma protein binding (91%), and ready formulation as a salt (pK_a 5.6) (Fig. 1*D*). The metabolic turnover of AWZ1066S by both liver microsomes and hepatocytes across a range of different species, including mouse, rat, dog, monkey, and human, is low and negatively correlated with species body size (*SI Appendix*, Table S3). High metabolic stability was also observed in the in vivo mouse PK profile (total clearance 0.47 $L{\cdot}h^{-1}{\cdot}kg^{-1}$ and $T_{1/2}$ 3.5 h) when dosed intravenously. The permeability of AWZ1066S in an LLC-PK1 cell assay is good (P_{app} 7.4×10^6 cm/s) and, despite being a mammalian P-gp transporter substrate (P-gp–mediated efflux ratio 7.8), AWZ1066S showed good to excellent oral bioavailability (range 54 to 91%) across a range of dosages up to 250 mg/kg in the mouse (*SI Appendix*, Table S4). AWZ1066S is a weak CYP2C9 inhibitor (IC_{50} 9.7 μM) and a weak CYP3A4 inducer (IC_{50} 37 μM) but does not show any time-dependent inhibition across five major human CYP450 isoforms (CYP1A, CYP2C9, CYP2C19, CYP2D6, CYP3A).

One of the major limitations of doxycycline, the current "gold standard" anti-*Wolbachia* macrofilaricide in the treatment of filariasis, is its prolonged treatment period of 4 to 6 wk to deliver a cure (6, 9, 10, 12). The community consensus is that novel macrofilaricide treatments need to be implementable in 7 d or less (5, 14). To assess if AWZ1066S could meet this demand, determined as a threshold reduction of *Wolbachia* >90% in 7 d, efficacy was evaluated in two independent animal models of filarial infection. As an initial screen, we used the adult *B. malayi* SCID mouse model (14). In this model, human bioequivalent exposures to 100 mg/d doxycycline require 6 wk to mediate >90% *Wolbachia* depletion within female *B. malayi* adult parasites, while the more potent second-generation tetracycline, minocycline, still requires a 4-wk exposure bioequivalent to 100 mg/d dosing to mediate similar efficacy (18, 19). AWZ1066S (100 mg/kg) reduced *Wolbachia* by 98% after only 7 d orally administered treatment (compared with the vehicle group) (Kruskal–Wallis statistic 50.7, $P < 0.0001$; Fig. 2*A*). Furthermore, the release of mf was completely prevented in 9/10 mice treated with AWZ1066S over the 6 wk of observation post treatment (*SI Appendix*, Table S5). We further investigated the preclinical efficacy of 7-d AWZ1066S dosing in a second rodent filarial infection system [*Litomosoides sigmodontis* gerbil model (20)]. After 7 d of twice-daily treatment of AWZ1066S at either 100 or 50 mg/kg orally, *Wolbachia* load was reduced by >99% compared with control untreated animals, 18 wk post treatment (Kruskal–Wallis statistic 43.5, $P < 0.0001$; Fig. 2*B*). In this model, mf produced by female adult worms circulate in the blood and thus peripheral microfilaremias can be tracked longitudinally post treatment. After AWZ1066S treatment, the peripheral blood microfilaremia began to decline from 6 wk post treatment. A state of amicrofilaremia (absence of mf in the blood) was evident from 14 wk post treatment in the 7-d AWZ1066S treatment groups, a state that was sustained until the end of the experiment at 18 wk post treatment. Thus, treatment with AWZ1066S for 7 d leads to sterilization and gradual depletion of mf with the assumption, based on extensive clinical trial data with doxycycline, that this will result in a "slow" killing of adult worms alongside an improved safety profile. Based on PK/PD (pharmacodynamic) modeling (21) of the available data, using human PK simulations, we predict that >90% of a patient population will achieve a 90% or higher *Wolbachia* reduction [considered fully efficacious clinically (8, 10, 22)] within 7 d using an oral dose of 10 mg/kg body weight of AWZ1066S in humans (Fig. 2*D* and *SI Appendix*, Table S6).

AWZ1066S was subsequently tested for safety pharmacology characteristics. AWZ1066S showed very low cytotoxicity in multiple in vitro toxicology assays (*SI Appendix*, Table S7). AWZ1066S was also tested against a panel of 25 well-characterized human protein assays (23) (CEREP panel) in vitro to assess secondary pharmacology. The CEREP panel screen results indicated low promiscuity across the panel (*SI Appendix*, Table S8). AWZ1066S was negative in both the Ames test and the in vivo micronucleus assay in the mouse (*SI Appendix*, Table S9). AWZ1066 was also evaluated for cardiovascular safety both in vitro (hERG and Nav1.5) and in vivo (anesthetized and conscious rats; *SI Appendix*, Table S10), demonstrating a low risk. In a preliminary 7-d dose range-finding study in the rat (*SI Appendix*, Table S11), the "no observed adverse effect level" for AWZ1066 was determined to be >300 mg/kg.

Discussion

The antibacterial activity profile of AWZ1066S was examined against a panel of clinically relevant bacterial strains, including gram-positive and gram-negative species and strains with known drug-resistance profiles. The data indicated that AWZ1066S is highly specific for *Wolbachia* (*SI Appendix*, Table S12). This high specificity of AWZ1066S against *Wolbachia* is a significant advantage, as it would predict minimal impact on the gut microbiota, lowering the risk of dysbiosis and the selection and emergence of resistance following administration to patients, in comparison with other anti-*Wolbachia*–based broad-spectrum antibiotic treatments.

In addition to the ability to elicit efficacy after 7 d of treatment, AWZ1066 also has a faster kill rate compared with other known antibiotics tested against *Wolbachia* in vitro. In a time-kill assay modified from the standard microfilaria assay, a panel of anti-*Wolbachia* drugs (24) including moxifloxacin, rifampicin, minocycline, doxycycline, and AWZ1066S was screened over a range of exposure intervals (1, 2, and 6 d). The results show AWZ1066S can achieve maximum reduction of *Wolbachia* just after 1 d of drug exposure compared with the other antibiotics tested (1 to 6 d of exposure; Fig. 3*A*). These results further support the potential of AWZ1066S to deliver treatment time frames of <7 d. Furthermore, differential time-to-kill profiles suggest a novel mode of action for the AWZ1066S class compared with antibiotics that work via inhibition of aspects of protein synthesis. Genetic approaches to identify the molecular target(s) of AWZ1066S have been thwarted by the intractability of this intracellular bacterium. However, using a proteomic approach with photoreactive chemical probes, we have identified a number of credible *Wolbachia* and host proteins that are being evaluated as potential drug targets of AWZ1066S (Fig. 3 *B* and *C* and Dataset S1).

In conclusion, starting with a hit chemotype from a modest-scale whole-cell screen, a medicinal chemistry-led scaffold hopping and multiparameter optimization program has delivered a first-in-class synthetic candidate molecule, AWZ1066S, that is highly specific against *Wolbachia*. Seven-day oral dosing regimens with AWZ1066S are capable of depleting *Wolbachia* >90% with sustained sterilization of microfilaria production in two independent filarial infection models. This candidate selected molecule meets all target candidate profile criteria for an anti-*Wolbachia* macrofilaricidal drug, and has entered formal preclinical evaluation. AWZ1066S has the potential to deliver a novel antifilarial therapy that could be deployed in target populations in a sub–7-day dosing regimen. The compound provides a unique opportunity to make a significant contribution to communities affected by filariasis, especially if the predicted macrofilaricidal effect can be confirmed in clinical trials.

Materials and Methods

The Chemical Characterization of AWB158, AWZ1066S and Its HCl Salt, and Photoreactive Probes 1 and 2. Please see *SI Appendix* for the synthesis of AWB158, AWZ1066S (and its HCl salt), and photoreactive probes 1 and 2.

N^2-isopropyl-N^4-(2-(trifluoromethyl)benzyl)quinazoline-2,4-diamine: AWB158. ^{1}H NMR (400 MHz, MeOD) δ 8.23 (d, J = 8.0 Hz, 1H), 7.89 to 7.81 (m, 1H), 7.78 (d, J = 7.8 Hz, 1H), 7.61 (t, J = 7.5 Hz, 1H), 7.56 to 7.42 (m, 4H), 5.11 (s, 2H), 4.18 to 4.06 (m, 1H), 1.13 (br, 6H); HRMS (ES) $C_{19}H_{20}N_4F_3$ $[M+H]^+$ requires 361.1640, found 361.1648; purity by HPLC 97.2%, R_t 9.255 min.

(S)-2-(3-methylmorpholino)-N-((2-(trifluoromethyl)pyridin-3-yl)methyl)pyrido[2,3-d]pyrimidin-4-amine: AWZ1066S. ^{1}H NMR (400 MHz, DMSO) δ 8.98 (t, J = 5.1 Hz, 1H), 8.70 (d, J = 4.4 Hz, 1H), 8.60 (d, J = 4.3 Hz, 1H), 8.50 (d, J = 8.0 Hz, 1H), 7.95 (d, J = 7.9 Hz, 1H), 7.64 (dd, J = 8.0, 4.6 Hz, 1H), 7.15 (dd, J = 8.0, 4.5 Hz, 1H), 4.94 (dd, J = 16.3, 4.7 Hz, 1H), 4.79 (dd, J = 16.3, 4.8 Hz, 1H), 4.45 (m, 1H), 4.21 (d, J = 13.1 Hz, 1H), 3.82 (d, J = 11.1 Hz, 1H), 3.58 (d, J = 11.3 Hz, 1H), 3.44 (d, J = 11.3 Hz, 1H), 3.32 to 3.23 (m, 1H), 2.99 (td, J = 13.2, 3.7 Hz, 1H), 0.87 (br, 3H); HRMS (ES) $C_{19}H_{19}N_6OF_3$ $[M+H]^+$ requires 405.1645, found 405.1641; purity by HPLC 97.8%, R_t 7.147 min. AWZ1066S HCl salt: ^{1}H NMR (400 MHz, DMSO) δ 10.49 (s, 1H), 9.24 (d, J = 7.8 Hz, 1H), 9.02 to 8.69 (m, 1H), 8.64 (d, J = 4.4 Hz, 1H), 8.05 (d, J = 7.9 Hz, 1H), 7.67 (dd, J = 7.9, 4.6 Hz, 1H), 7.52 (dd, J = 7.8, 5.6 Hz, 1H), 4.97 (dd, J = 15.9, 4.4 Hz, 1H), 4.88 (dd, J = 15.9, 3.9 Hz, 1H), 4.50 (m, 1H), 4.26 (d, J = 13.1 Hz, 1H), 3.88 (d, J = 10.1 Hz, 1H), 3.62 (t, J = 17.2 Hz, 1H), 3.55 to 3.13 (m, 4H), 0.98 (br, 3H).

2-(1-(4-(((2-(trifluoromethyl)pyridin-3-yl)methyl)amino)pyrido[2,3-d]pyrimidin-2-yl)piperidin-4-yl)ethyl (2-(3-(but-3-yn-1-yl)-3H-diazirin-3-yl)ethyl)carbamate: photoreactive probe 1. ^{1}H NMR (400 MHz, $CDCl_3$) δ 8.75 (d, J = 4.3 Hz, 1H), 8.61 (d, J = 4.4 Hz, 1H), 7.94 (d, J = 7.7 Hz, 1H), 7.86 (d, J = 7.9 Hz, 1H), 7.44 (dd, J = 7.9, 4.7 Hz, 1H), 6.98 (dd, J = 7.9, 4.5 Hz, 1H), 6.10 (t, J = 5.4 Hz, 1H), 5.02 (d, J = 5.6 Hz, 2H), 4.90 to 4.73 (m, 2H), 4.11 (t, J = 6.2 Hz, 2H), 3.05 (dd, J = 12.0, 5.7 Hz, 2H), 2.83 (t, J = 12.2 Hz, 2H), 2.10 to 1.88 (m, 2H), 1.80 to 1.62 (m, 7H), 1.59 to 1.47 (m, 4H), 1.10 (br, 2H); HRMS (ES) $C_{29}H_{33}N_9O_2F_3$ $[M+H]^+$ requires 596.2704, found 596.2709; purity by HPLC 90.3%, R_t 8.888 min.

2-(1-(4-(((2-(trifluoromethyl)pyridin-3-yl)methyl)amino)pyrido[2,3-d]pyrimidin-2-yl)piperidin-4-yl)ethyl (1-oxo-1-((4-(3-(trifluoromethyl)-3H-diazirin-3-yl)benzyl)amino)pent-4-yn-2-yl)carbamate: photoreactive probe 2. ^{1}H NMR (400 MHz, $CDCl_3$) δ 8.75 (d, J = 4.3 Hz, 1H), 8.61 (d, J = 4.3 Hz, 1H), 8.04 to 7.86 (m, 2H), 7.44 (dd, J = 7.9, 4.6 Hz, 1H), 7.31 (d, J = 8.3 Hz, 2H), 7.14 (d, J = 8.1 Hz, 2H), 6.99 (dd, J = 8.0, 4.5 Hz, 1H), 6.75 (br, 1H), 6.27 (br, 1H), 5.65 (br, 1H), 5.02 (d, J = 5.4 Hz, 2H),

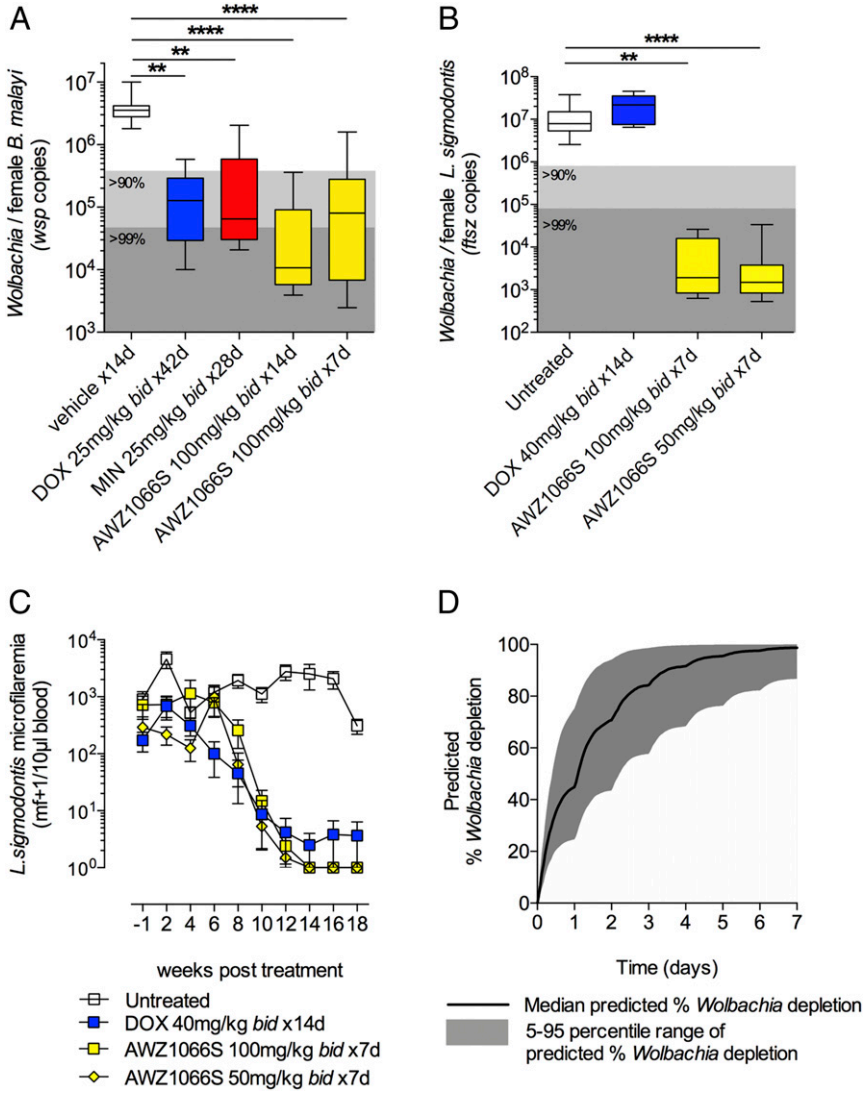


Fig. 2. In vivo anti-*Wolbachia* efficacy of AWZ1066S. (*A* and *B*) Anti-*Wolbachia* efficacy against female adult-stage *B. malayi* in SCID mice (*A*) or *L. sigmodontis* in gerbils (*B*) after doxycycline (DOX), minocycline (MIN), or AWZ1066S oral treatments at the indicated doses. Tail and whisker plots are minimum, 25th, median, 75th, and maximum *Wolbachia wsp* or *ftsz* copy number per female worm in samples of 5 to 24 worms derived from groups of four to nine animals from an individual experiment. Significant differences compared with vehicle/untreated are indicated ****$P < 0.0001$, **$P < 0.01$ (Kruskal–Wallis with Dunn's tests for intergroup *Wolbachia* variation). bid, twice a day. (*C*) Longitudinal effects on circulating *L. sigmodontis* microfilaremias −1 to 18 wk after DOX or AWZ1066S oral treatments at the indicated doses in gerbils. (*D*) Result of PK/PD Monte Carlo prediction of clinical activity of AWZ1066S when dosed at 600 mg given predicted PK properties in humans and established in vitro PD properties against *Wolbachia*.

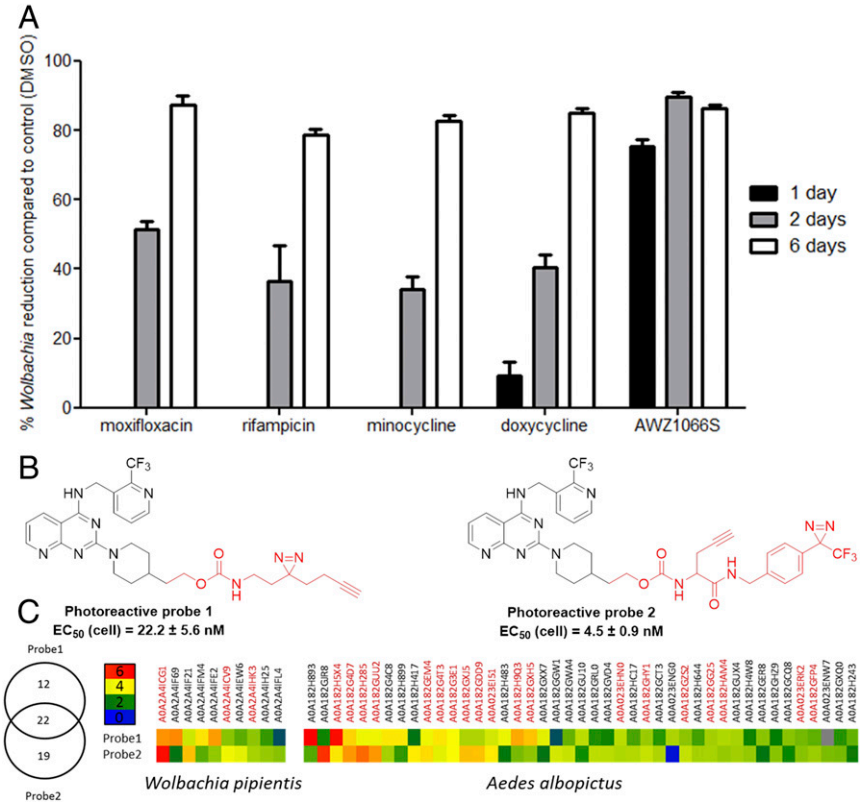


Fig. 3. Unique mode of action of AWZ1066S was indicated by its fast kill rate and was investigated through a proteomic target identification approach using two photoreactive chemical probes. (*A*) The *Wolbachia* depletion rates of AWZ1066S measured for three different treatment lengths (1, 2, and 6 d) in the *B. malayi* microfilaria time-kill assay. Doxycycline, minocycline, moxifloxacin, and rifampicin were used as positive controls (only doxycycline for day 1). Data are expressed as mean ± SD of five replicates for each time point. (*B*) Two photoreactive chemical probes used for target identification of AWZ1066S in *Wolbachia*. Structures (bifunctional, photoreactive, and clickable side chains are highlighted in red) and their anti-*Wolbachia* activity in the cell assay ($n = 3$). (*C*) Fifty-three putative protein targets of photoreactive probes 1 and 2 assigned (as shown in the Venn diagram) based on statistical testing [right-sided *t* test, permutation-based false discovery rate = 0.001, Artificial within groups variance (S0) = 3] of label-free quantification (LFQ) intensities measured in samples derived from probe-treated cells and control, DMSO-treated cells ($n = 3$). Protein targets presented in the left-hand block are from *W. pipientis* and in the right-hand block are from *A. albopictus*. Numbers within the heatmap legend represent Log_2 LFQ *t* test differences. Protein ID codes above the heatmap given in red indicate 22 proteins identified as common targets of both probes.

4.91 to 4.72 (m, 2H), 4.67 to 4.44 (m, 2H), 4.41 to 4.27 (m, 1H), 4.19 to 4.06 (m, 2H), 3.64 (s, 1H), 2.94 to 2.73 (m, 3H), 2.65 (ddd, $J = 17.0, 6.9, 2.6$ Hz, 1H), 2.09 (t, $J = 2.6$ Hz, 1H), 1.78 to 1.66 (m, 2H), 1.59 to 1.41 (m, 2H), 1.14 to 0.96 (m, 2H); HRMS (ES) $C_{36}H_{35}N_{10}O_3F_6$ $[M+H]^+$ requires 769.2792, found 769.2796; purity by HPLC 91.0%, R_t 9.561 min.

In Vitro Anti-*Wolbachia* Cell-Based Screening. Anti-*Wolbachia* activity was assessed in the A·WOL high-content imaging assay as described previously (17). In brief, this utilized a mosquito (*A. albopictus*)-derived cell line (C6/36), stably infected with *Wolbachia pipientis* (*w*AlbB) with a readout of the percentage of the cells infected with *Wolbachia*. The EC_{50} values reported were the means of at least five individual experiments.

In Vitro Anti-*Wolbachia B. malayi* Microfilaria Assay and Time-Kill Assay. *B. malayi* mf were obtained from patently infected *Meriones unguiculatus* gerbils as described previously (25). A series dilution of compounds (five concentrations) were incubated with 8,000 mf per well (five replicates) in RPMI supplemented with 10% FBS, 1% penicillin streptomycin, and 1% amphotericin B. After a 6-d incubation (37 °C, 5% CO_2), motility was assessed by microscopy and DNA was extracted for quantitative PCR (qPCR) analysis to obtain ratios of *Wolbachia* surface protein copy number (*wsp*) to GST copy number (*gst*), as previously described (26). Time-kill assays were completed using the same method with the exception of a wash step on the indicated day. The drug concentration in the time-kill assay was 10 times that of the EC_{50}. There were five replicates per time point per drug treatment. The EC_{50} values or *Wolbachia* reduction percentages reported were from one individual experiment.

In Vitro Drug Metabolism/Pharmacokinetic Assays. The DMPK property data described above were measured once through a high-throughput platform provided by AstraZeneca UK. The methods of the five assays, including $LogD_{7.4}$, aqueous solubility, plasma protein binding, and microsome and hepatocyte clearance measurements, have been reported previously (27, 28).

In Vivo Anti-*Wolbachia* Pharmacodynamic Studies.

Animals. For *B. malayi* studies, inbred male SCID CB.17 mice and outbred *M. unguiculatus* gerbil breeding pairs were purchased from Charles River, Europe. Rodents were maintained/bred in specific pathogen-free conditions at the University of Liverpool Biological Services Unit. All experiments were approved by the animal welfare ethics committees of the University of Liverpool and Liverpool School of Tropical Medicine. Studies were conducted in accordance with Home Office legislation. Experiments with *L. sigmodontis* were performed at the Institute for Medical Microbiology, Immunology and Parasitology, University Hospital Bonn in accordance with European Union animal welfare guidelines, and all protocols were approved by the Landesamt für Natur, Umwelt und Verbraucherschutz (AZ 84-02.04.2015.A507). Female *M. unguiculatus* gerbils were obtained from Janvier Labs and housed at the animal facility of the Institute for Medical Microbiology, Immunology and Parasitology in individually ventilated cages on a 12-h light/dark cycle with food and water ad libitum.

Filarial experimental infections. Infective-stage *B. malayi* L3 larvae were propagated as previously described (14). Male mice 6 to 12 wk of age ($n = 5$ to 9) or male gerbils ($n = 6$) 8 to 16 wk of age were infected with *B. malayi* L3 i.p. (50 or 100× L3 mouse, 400× L3, gerbil). Mouse experimental infections were maintained for 13 wk, while gerbil infections were maintained for a

maximum of 12 mo. Motile *B. malayi* parasites were recovered by peritoneal lavage at necropsy and enumerated by microscopy. Motile mf from gerbil infections were periodically isolated by i.p. catheter drain under anesthesia with recovery as previously described (14).

For *L. sigmodontis* infection, 6- to 8-wk-old female gerbils were exposed to *Ornithonyssus bacoti* mites containing infective-stage *L. sigmodontis* L3. Treatment of microfilaremic gerbils started 13 wk following infection. Necropsies occurred 18 wk following the start of treatment. At necropsy, *L. sigmodontis* worms were isolated from the serous cavities and quantified as previously described (29). For microfilaria counts, 10 μL of peripheral blood was taken from the saphenous vein in biweekly intervals starting at 12 wk post infection and diluted in 300 μL of Hinkelmann solution (0.5% eosin Y, 0.5% phenol, 0.185% formaldehyde in aqua dest). After centrifugation at 400 × *g* for 5 min, the supernatant was discarded; the pellet was resuspended in 1 mL and transferred to a 1-mL Sedgewick Rafter Counting Chamber to quantify total mf using a microscope.

Drug dosing. Infected animals were randomly assigned to dose groups ($n = 5$ to 9). AWZ1066S (or it HCl salt) was dissolved in PEG300/propylene glycol/H_2O (55/25/20). Minocycline and doxycycline hyclate (Sigma-Aldrich) were dissolved in water. Animals were weighed, and weight-corrected volumes of dosing solution were administered by oral gavage (mouse: 100 μL/25 g body weight; gerbil: 2.5 mL/kg).

Molecular assays. For *B. malayi* infections, determination of *Wolbachia* single-copy *wsp* gene quantity was undertaken by qPCR as previously described (14, 18) whereas, for *L. sigmodontis*, *Wolbachia* was determined by FtsZ qPCR as previously described (30). Between 5 and 20 individual worms were assayed, derived from dose groups of three to nine animals.

Statistical analysis. Continuous variables (*Wolbachia* loads, adult worm burdens, microfilaria burdens) were tested for normal distribution by D'Agostino and Pearson omnibus normality tests pre and post Log_{10} transformation. Variables did not satisfy the assumption of normality and were compared by two-tailed Kruskal–Wallis tests with Dunn's multiple tests, post hoc. Post hoc testing scrutinized drug groups compared with vehicle or untreated controls. Significance levels are indicated as $*P < 0.05$, $**P < 0.01$, $***P < 0.001$, and $****P < 0.0001$. All statistics were undertaken using GraphPad Prism v6 software.

PK/PD predictions of AWZ1066S activity in clinical settings. The predicted human pharmacokinetic parameters (*SI Appendix*, Table S6) were used to predict the activity of AWZ1066S when administered in humans for 1 wk using the simulator tool in Pmetrics (31). As previously described (21), we used a PK/PD model which links predicted human pharmacokinetic parameters with the observed in vitro activity of the drug against intracellular *Wolbachia*. One thousand subjects were simulated and the % of subjects achieving >90% *Wolbachia* reduction at each week was recorded, and data are presented as the cumulative number of patients who achieved >90% *Wolbachia* load reduction.

Preliminary Target Pull-Down Using Photoreactive Probes with *Wolbachia*-Infected Cells. Please see *SI Appendix* for experimental details of sample preparation and pull-down for proteomics and LC-MS/MS analysis of proteomic samples and data processing.

Data Availability Statement. The authors declare that the data supporting the findings in this manuscript are available within the paper and its *SI Appendix*. The raw data related to the studies described in this manuscript are available from the corresponding authors upon reasonable request.

ACKNOWLEDGMENTS. We thank Marianne Koschel, Iliana Johannes, Martina Fendler, and Venelin Nikolov for their technical support with the *L. sigmodontis* gerbil studies. We thank the National Collection for Type Cultures (Public Health England), David Wareham (Blizard Institute, Queen Mary University of London), and Haitham Hussain (University College London Eastman Dental Institute) for provision of bacterial strains. The A·WOL Consortium is supported by grants (OPP1054324, A·WOL II and III) from The Bill & Melinda Gates Foundation awarded to the Liverpool School of Tropical Medicine. This work was also supported by Grant GHIT-RFP-2013-002 from the Global Health Innovative Technology (GHIT) Fund (to F.G., P.M.O., M.J.T., and S.A.W.). Experiments performed in Bonn and at Wuxi AppTec were supported by The Bill & Melinda Gates Foundation through the Macrofilaricidal Drug Accelerator Initiative.

1. Taylor MJ, Hoerauf A, Bockarie M (2010) Lymphatic filariasis and onchocerciasis. *Lancet* 376:1175–1185.
2. Bockarie MJ, Deb RM (2010) Elimination of lymphatic filariasis: Do we have the drugs to complete the job? *Curr Opin Infect Dis* 23:617–620.
3. Mackenzie CD, Homeida MM, Hopkins AD, Lawrence JC (2012) Elimination of onchocerciasis from Africa: Possible? *Trends Parasitol* 28:16–22.
4. Taylor MJ, Bandi C, Hoerauf A (2005) *Wolbachia* bacterial endosymbionts of filarial nematodes. *Adv Parasitol* 60:245–284.
5. Boussinesq M, Fobi G, Kuesel AC (2018) Alternative treatment strategies to accelerate the elimination of onchocerciasis. *Int Health* 10:i40–i48.
6. Taylor MJ, et al. (2005) Macrofilaricidal activity after doxycycline treatment of *Wuchereria bancrofti*: A double-blind, randomised placebo-controlled trial. *Lancet* 365: 2116–2121.
7. Turner JD, et al. (2006) A randomized, double-blind clinical trial of a 3-week course of doxycycline plus albendazole and ivermectin for the treatment of *Wuchereria bancrofti* infection. *Clin Infect Dis* 42:1081–1089.
8. Debrah AY, et al. (2007) Macrofilaricidal effect of 4 weeks of treatment with doxycycline on *Wuchereria bancrofti*. *Trop Med Int Health* 12:1433–1441.
9. Hoerauf A, et al. (2008) *Wolbachia* endobacteria depletion by doxycycline as antifilarial therapy has macrofilaricidal activity in onchocerciasis: A randomized placebo-controlled study. *Med Microbiol Immunol (Berl)* 197:295–311, and erratum (2008) 197: 335.
10. Turner JD, et al. (2010) Macrofilaricidal activity after doxycycline only treatment of *Onchocerca volvulus* in an area of *Loa loa* co-endemicity: A randomized controlled trial. *PLoS Negl Trop Dis* 4:e660.
11. Tamarozzi F, et al. (2012) Long term impact of large scale community-directed delivery of doxycycline for the treatment of onchocerciasis. *Parasit Vectors* 5:53.
12. Walker M, et al. (2015) Therapeutic efficacy and macrofilaricidal activity of doxycycline for the treatment of river blindness. *Clin Infect Dis* 60:1199–1207.
13. Johnston KL, Ford L, Taylor MJ (2014) Overcoming the challenges of drug discovery for neglected tropical diseases: The A·WOL experience. *J Biomol Screen* 19:335–343.
14. Halliday A, et al. (2014) A murine macrofilaricide pre-clinical screening model for onchocerciasis and lymphatic filariasis. *Parasit Vectors* 7:472.
15. Johnston KL, et al. (2017) Identification and prioritization of novel anti-*Wolbachia* chemotypes from screening a 10,000-compound diversity library. *Sci Adv* 3:eaao1551.
16. Hong WD, et al. (2018) Anti-*Wolbachia* compounds. International Bureau (IB) Patent WO2018134685.
17. Clare RH, et al. (2015) Development and validation of a high-throughput anti-*Wolbachia* whole-cell screen: A route to macrofilaricidal drugs against onchocerciasis and lymphatic filariasis. *J Biomol Screen* 20:64–69.
18. Sharma R, et al. (2016) Minocycline as a re-purposed anti-*Wolbachia* macrofilaricide: Superiority compared with doxycycline regimens in a murine infection model of human lymphatic filariasis. *Sci Rep* 6:23458, and erratum (2018) 8:46934.
19. Turner JD, et al. (2017) Albendazole and antibiotics synergize to deliver short-course anti-*Wolbachia* curative treatments in preclinical models of filariasis. *Proc Natl Acad Sci USA* 114:E9712–E9721.
20. Hübner MP, Torrero MN, McCall JW, Mitre E (2009) *Litomosoides sigmodontis*: A simple method to infect mice with L3 larvae obtained from the pleural space of recently infected jirds (*Meriones unguiculatus*). *Exp Parasitol* 123:95–98.
21. Aljayyoussi G, et al. (2017) Short-course, high-dose rifampicin achieves *Wolbachia* depletion predictive of curative outcomes in preclinical models of lymphatic filariasis and onchocerciasis. *Sci Rep* 7:210, and erratum (2018) 8:1384.
22. Debrah AY, et al. (2011) Macrofilaricidal activity in *Wuchereria bancrofti* after 2 weeks treatment with a combination of rifampicin plus doxycycline. *J Parasitol Res* 2011:201617.
23. Bowes J, et al. (2012) Reducing safety-related drug attrition: The use of in vitro pharmacological profiling. *Nat Rev Drug Discov* 11:909–922.
24. Johnston KL, et al. (2014) Repurposing of approved drugs from the human pharmacopoeia to target *Wolbachia* endosymbionts of onchocerciasis and lymphatic filariasis. *Int J Parasitol Drugs Drug Resist* 4:278–286.
25. Griffiths KG, Alworth LC, Harvey SB, Michalski ML (2010) Using an intravenous catheter to carry out abdominal lavage in the gerbil. *Lab Anim (NY)* 39:143–148.
26. McGarry HF, Egerton GL, Taylor MJ (2004) Population dynamics of *Wolbachia* bacterial endosymbionts in *Brugia malayi*. *Mol Biochem Parasitol* 135:57–67.
27. Basarab GS, et al. (2014) Optimization of pyrrolamide topoisomerase II inhibitors toward identification of an antibacterial clinical candidate (AZD5099). *J Med Chem* 57:6060–6082.
28. Doyle K, et al. (2016) Discovery of second generation reversible covalent DPP1 inhibitors leading to an oxazepane amidoacetonitrile based clinical candidate (AZD7986). *J Med Chem* 59:9457–9472.
29. Ajendra J, et al. (2016) NOD2 dependent neutrophil recruitment is required for early protective immune responses against infectious *Litomosoides sigmodontis* L3 larvae. *Sci Rep* 6:39648.
30. Schiefer A, et al. (2012) Corallopyronin A specifically targets and depletes essential obligate *Wolbachia* endobacteria from filarial nematodes in vivo. *J Infect Dis* 206: 249–257.
31. Neely MN, van Guilder MG, Yamada WM, Schumitzky A, Jelliffe RW (2012) Accurate detection of outliers and subpopulations with Pmetrics, a nonparametric and parametric pharmacometric modeling and simulation package for R. *Ther Drug Monit* 34: 467–476.